Molecular Therapy
Nucleic Acids
Original Article

circHMCU Promotes Proliferation and Metastasis of Breast Cancer by Sponging the let-7 Family

Xiaojin Song,[1] Yiran Liang,[1] Yuting Sang,[1] Yaming Li,[1] Hanwen Zhang,[1] Bing Chen,[2] Lutao Du,[3] Ying Liu,[1] Lijuan Wang,[2] Wenjing Zhao,[2] Tingting Ma,[1] Chuanxin Wang,[3] and Qifeng Yang[1,2]

[1]Department of Breast Surgery, School of Medicine, Qilu Hospital, Shandong University, Wenhua West Road No. 107, Ji'nan, Shandong 250012, P.R. China; [2]Pathology Tissue Bank, Qilu Hospital, Shandong University, Ji'nan, Shandong 250012, P.R. China; [3]Department of Clinical Laboratory, The Second Hospital of Shandong University, No. 247 Beiyuan Street, Ji'nan, Shandong 250033, P.R. China

Circular RNA (circRNA), as a kind of novel identified non-coding RNA, has become the focus of attention for its vital physiological and pathological roles. However, the function and mechanism of circRNAs in the regulation of cancer progression are largely unknown. In the present study we found a circRNA termed circHMCU whose expression was associated with poor prognosis. It was upregulated in cell lines with high metastatic potential compared with its parental cell line and in breast cancer tissues compared with normal tissues. *In vitro* results proved that circHMCU could significantly promote proliferation, migration, and invasion abilities of breast cancer cells via affecting the G_1 phase cell cycle checkpoint and the epithelial-mesenchymal transition (EMT) pathway. Further *in vivo* studies showed that overexpression of circHMCU contributed to rapid proliferation and lung metastasis of breast cancer. For determination of the mechanisms, bioinformatics analysis revealed two complementary sequences within circHMCU for let-7 microRNAs, which was validated by a luciferase reporter assay. Finally, let-7 microRNAs could rescue the functions of circHMCU in breast cancer via suppressing the expression of MCY, HMGA2, and CCND1. Taken together, our findings demonstrated that circHMCU exerted oncogenic functions in breast cancer and could be a used as a novel biomarker in the diagnosis and prognosis of breast cancer.

INTRODUCTION

Breast cancer is the most common cancer among women and one of the leading causes of cancer-related mortality worldwide, with an estimated 1.7 million cases and 521,900 deaths in 2012, which accounts for 25% of all cancer cases and 15% of all cancer deaths among females.[1] Breast cancer is a heterogeneous disease, with both genetic and epigenetic changes being essential for breast cancer initiation, development, metastasis, and drug resistance. During the past decades, studies revealed that non-coding RNAs were involved in all aspects of the process of carcinogenesis and could be used as biomarkers for early risk stratification and the prediction of long-term survival. However, the association and underlying mechanisms between these non-coding RNAs and cancer remain elusive. Therefore, further understanding is warranted to illuminate the function and clinical significance of non-coding RNAs.

Circular RNAs (circRNAs) represent a new class of non-coding RNA molecules with 3′ and 5′ ends covalently linked in a closed-loop structure, in contrast to the typical linear RNAs with 5′ caps and 3′ poly(A) tails. In the 1990s, a few circRNAs were identified in humans and rodents, but they were considered as products of mis-splicing events.[2] However, recent high-throughput sequencing and novel computational approaches have shown that the expression of circRNAs is widespread,[3] and many circRNAs are predominantly localized in the cytoplasm, indicating important functions for circRNAs in human diseases.[4] Han et al.[5] reported that the circRNA circMTO1 is significantly downregulated in hepatocellular carcinoma (HCC) tissues and closely related to the prognosis of breast cancer patients. Zhang et al.[6] reported that circLARP4 was downregulated in gastric cancer (GC) tissues and represented an independent prognostic factor for overall survival of GC patients. However, their biogenesis processes and potential function are poorly understood. Recently, studies have shown that circRNA molecules are enriched with microRNA (miRNA) recognition elements (MREs) and can function as miRNA sponges; for example, as ciRS-7 served as a miR-7 sponge,[7] circHIPK3 served as a miR-124 sponge,[8] and circ-ITCH served as a miR-17/miR-224 sponge.[9]

In the present study, we uncovered the promoting effect that circHMCU played in breast cancer, and the competitive endogenous RNA (ceRNA) networks as well as potential targeting relationships were constructed according to bioinformatics predictions. A significantly upregulated expression of circHMCU was detected in breast

Received 16 February 2020; accepted 27 March 2020;
https://doi.org/10.1016/j.omtn.2020.03.014.

Correspondence: Qifeng Yang, Department of Breast Surgery, School of Medicine, Qilu Hospital, Shandong University, Wenhua West Road No. 107, Ji'nan, Shandong 250012, P.R. China.
E-mail: qifengy_sdu@163.com

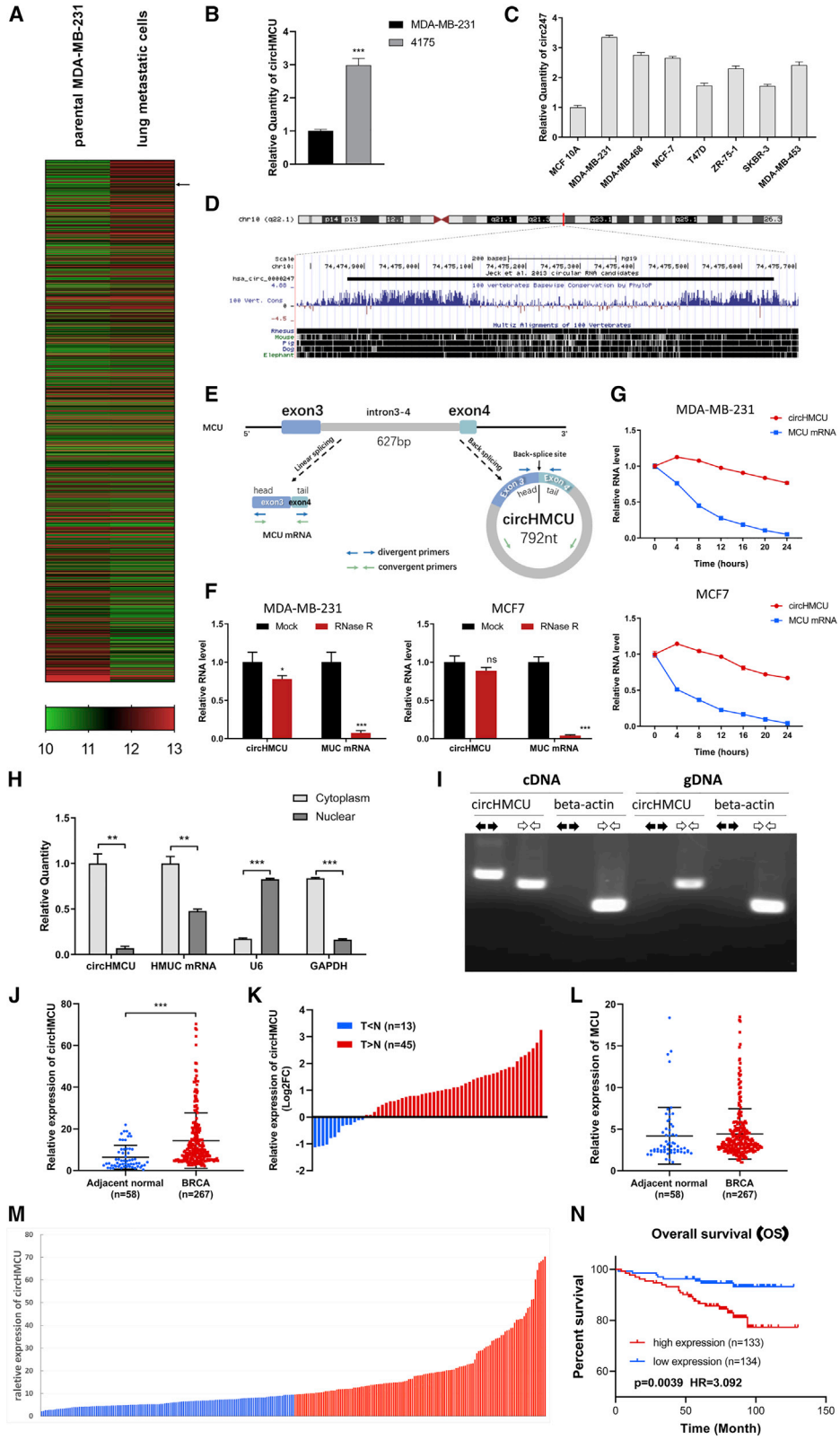

(legend on next page)

cancer cell lines with high lung metastatic ability. Then, we examined the functions and mechanisms of circHMCU using breast cancer cell lines. We found that circHMCU could promote cell proliferation and metastasis and bind to miRNA let-7 family members, thus increasing the expression of let-7 family target genes such as MYC, HMGA2 and CCND1. Our study revealed the cancer-promoting role of circHMCU and helped to elucidate the epigenetic mechanism of carcinogenesis and metastasis of breast cancer, which may facilitate the development of effective clinical treatments and early diagnosis for breast cancer patients.

RESULTS

Identification and Characteristics of circHMCU (hsa_circ_0000247) in Breast Cancer

Breast cancer is a heterogeneous disease, and metastasis is one of the main factors influencing prognosis of breast cancer patients. To investigate circRNAs associated with the metastasis of breast cancer, the GEO database (GEO: GSE111504) was reanalyzed. We compared the expression profiles of circRNAs in parental MDA-MB-231 cells and lung metastatic cells (LM2), and only circRNAs with high abundance were included for further analysis (Figure 1A). We found that the expression of hsa_circ_0000247 (circRNA derived from the human MCU gene) was upregulated in lung metastasis sublines (LM2). RT-PCR was then performed in MDA-MB-231- and MDA-MB-231-derived cell line 4175 with higher metastatic abilities, and the result was inconsistent with that from the GEO database (Figure 1B), suggesting that circHMCU may play a role in the metastasis of breast cancer. Furthermore, circHMCU was upregulated in breast cancer cells compared with normal breast epithelial MCF-10A cells (Figure 1C). circHMCU is located in chromosome 10, 792 bp in length, with high conservation in vertebrates (Figure 1D). It consists of 2 exons (exons 3 and 4) as well as the intron between them. This fragment forming circHMCU is flanked by long introns on each side (Figure 1E). Because of the naturally closed-loop structure, circRNA could be more resistant to exonuclease treatment such as RNase R digestion and thus could be more stable than linear RNA (for example, mRNA). As shown in Figure 1F, circHMCU had higher resistance to the treatment of RNase R while the linear mRNA of its host gene MCU could be digested. To further confirm the circular characteristics of circHMCU, we added actinomycin D (ActD), an inhibitor of transcription in MDA-MB-231 and MCF-7 cells, or DMSO as a negative control (NC). As expected, circHMCU was more stable and resistant to ActD treatment (Figure 1G). Subsequently, gel electrophoresis was used to confirm the head-to-tail splicing in the PCR product of circHMCU. We designed convergent primers that could amplify both MCU mRNA and circRNA, and divergent primers that could only amplify circHMCU. Using cDNA and genomic DNA (gDNA) from MCF-7 breast cancer cell lines as templates, circHMCU was only amplified by divergent primers in cDNA, and no amplification product was observed in gDNA (Figure 1I). To explore the cellular distribution of circHMCU, the expression levels of cytoplasmic control transcripts (GAPDH), nuclear control transcript (U6), and circHMCU were examined by qRT-PCR in the cytoplasmic and nuclear fractions of MCF7 cells. The results showed that circHMCU was predominantly expressed in the cytoplasm (Figure 1H), which was inconsistent with the results of fluorescence *in situ* hybridization (FISH) (Figure S1).

To confirm whether circHMCU could play a role in breast cancer progression, qRT-PCR was performed in 58 pairs of breast cancer tissues and adjacent normal breast tissues, and we found that circHMCU was obviously increased in the breast cancer tissues compared with normal breast tissues (Figures 1J and 1K). Interestingly, the linear isoform of its host gene, MCU, showed no significant upregulation in breast cancer tissues compared with adjacent normal breast tissues (Figure 1L), suggesting that the biological function of circHMCU was independent from the linear mRNA isoform. For survival analysis, the 267 breast cancer patients were divided into two groups according to the median expression level of circHMCU, with 133 cases in the high expression group and 134 cases in the low expression group (Figure 1M). The Kaplan-Meier survival curve in Figure 1N shows that the high circHMCU expression was significantly correlated with a poor prognosis in breast cancer patients ($p = 0.039$, hazard ratio [HR] = 3.092). We further explored the correlation between circHMCU and clinicopathological parameters and found that the level of circHMCU was positively correlated with histological grade ($p = 0.013$), lymph node metastasis ($p = 0.017$), T (tumor) stage ($p = 0.002$), and N (node) stage ($p = 0.009$) (Table 1). These results suggest that circHMCU may play an essential role in tumor progression of breast cancer.

Figure 1. Identification and Characteristics of circHMCU (hsa_circ_0000247) in Breast Cancer

(A) The cluster heatmap shows the differentially expressed circRNAs between parental MDA-MB-231 and lung metastatic cells. Red indicates a high expression level, and green indicates a low expression level. The arrow indicates circHMCU. (B) Expression level of circHMCU in MDA-MB-231 and its derivative (4175). (C) circHMCU expression in normal breast epithelial cells and breast cancer cell lines. (D) circHMCU is derived from the third and fourth exons as well as the intron between them from the human MCU gene, which is located on chromosome 10. (E) Scheme illustrating the production of circHMCU. Arrow represents "head-to-tail" splicing sites of circHMCU. (F) Quantitative real-time PCR analysis of circHMCU and MCU mRNA after RNase R treatment. (G) Quantitative real-time PCR analysis of circHMCU and MCU mRNA after ActD treatment. DMSO treatment was performed as a negative control. (H) Quantitative real-time PCR analysis of circHMCU and MCU mRNA in the cytoplasm or the nucleus in MCF-7 cells. (I) The existence of circHMCU was validated in breast cancer cells by PCR. Divergent primers amplified circHMCU in cDNA but not genomic DNA (gDNA). β-Actin was used as negative control. (J) The expression level of circHMCU was increased in breast cancer tissues (n = 267) compared with normal breast tissues (n = 58). (K) 77.59% (43/58) breast cancer patients presented increased expression of circHMCU. The bar chart presents the $\log_2$FC (fold change). (L) Expression level of MCU (linear isoform) in breast cancer tissues (n = 267) compared with normal breast tissues (n = 58). (M) According to the median expression level of circHMCU, the 267 breast cancer patients were divided into two groups. The blue bars represent the low-expression group, and the red bars represent the high-expression group. (N) Kaplan-Meier analysis of the association between circHMCU expression and prognosis of breast cancer patients. Data are the means ± SEM of three experiments. $^{**}p < 0.01$, $^{***}p < 0.001$.

Table 1. Clinicopathological Variables and circHMCU Expression in 267 Breast Cancer Patients

Variables	Classifier	Low circHMCU (n = 134)	High circHMCU (n = 133)	Total	p Value
Age	≤50	71	74	145	0.755
	>50	63	59	122	
Menopause	no	73	64	137	0.359
	yes	61	69	130	
Histologic grade	I	8	1	9	
	II	93	84	177	0.013
	III	33	48	81	
Lymph node metastasis	no	82	61	143	0.017
	yes	52	72	124	
T stage	T1	78	49	127	
	T2	53	79	132	0.002
	T3/T4	3	5	8	
N stage	N0	82	61	140	
	N1/N2	51	65	122	0.009
	N3	1	7	5	
ER	negative	15	39	54	<0.001
	positive	119	94	213	
PR	negative	24	42	66	0.014
	positive	110	91	201	
HER2	negative	106	84	190	0.006
	positive	28	49	77	
Molecular subtype	TNBC	10	21	31	0.053
	non-TNBC	124	112	236	
Ki-67 scores	low	42	31	73	0.182
	high	92	102	194	

T, tumor; N, node; ER, estrogen receptor; PR, progesterone receptor; HER2, human epidermal growth factor receptor-2.

Effects of circHMCU on Breast Cancer Cell Cycle, Proliferation, and Apoptosis *In Vitro*

In an attempt to investigate the biological functions of circHMCU in breast cancer cells, we designed interference sequences targeting the junction sites of circHMCU that could only downregulate the expression of circHMCU but not the linear mRNA of the MCU gene (Figure 2A). The silencing efficiency was confirmed by quantitative real-time PCR (Figure 2B; Figure S2A). Meanwhile, we transfected the empty plasmid pLCDH and the circHMCU overexpression plasmid pLCDH-circHMCU to breast cancer cell lines (MDA-MB-231, MCF-7, and SKBR3) for the ectopic expression of circHMCU, and the overexpression efficiency was confirmed by quantitative real-time PCR (Figure 2C; Figure S2A). The three cell lines we used (MDA-MB-231, MCF-7, and SKBR3) represent breast cancer with different hormone receptor and Her2 status. A 3-(4,5-dimethylthiazol-2-yl)-2,5-dimethyltetrazolium bromide (MTT) assay showed that the proliferation rate was significantly upregulated in circHMCU cells in comparison with control cells transfected with pLCDH-ciR (Figure 2D; Figure S2B), both in hormone receptor-positive and -negative and human epidermal growth factor receptor-2 (HER2)-positive and -negative cell lines. A colony formation assay indicated that stable overexpression of circHMCU significantly increased the proliferation rate of breast cancer cell lines MDA-MB-231 and MD-MB-468 (Figure 2E). Consistently, an EdU (5-ethynyl-2′-deoxyuridine) incorporation assay showed that the proliferation of MDA-MB-231, MD-MB-468, and SKBR3 cells was strengthened by transfection with circHMCU overexpression plasmid (Figure 2G; Figure S2C). Furthermore, flow cytometry was performed to evaluate the effect of circHMCU on cell proliferation. A cell cycle assay revealed that inhibiting the expression of circHMCU could induce G_0/G_1 arrest by increasing the fraction of the G_0/G_1 phase, as compared with that of the control cells (Figure 2H). Western blot was then performed to prove that circHMCU knockdown could decrease the expression of cyclin B1, cyclin D1, cyclin D3, CDK4, and CDK6 (Figure 2I). We then examined the effects of circHMCU on the apoptosis of breast cancer cells transfected with small interfering RNAs (siRNAs) targeting the back-splice junction of circHMCU (circHMCU-si) or circHMCU overexpression vector by flow cytometry. The result showed that the apoptosis rate increased from 8.52% to 13.7% in MDA-MB-468 cells (Figure 2F).

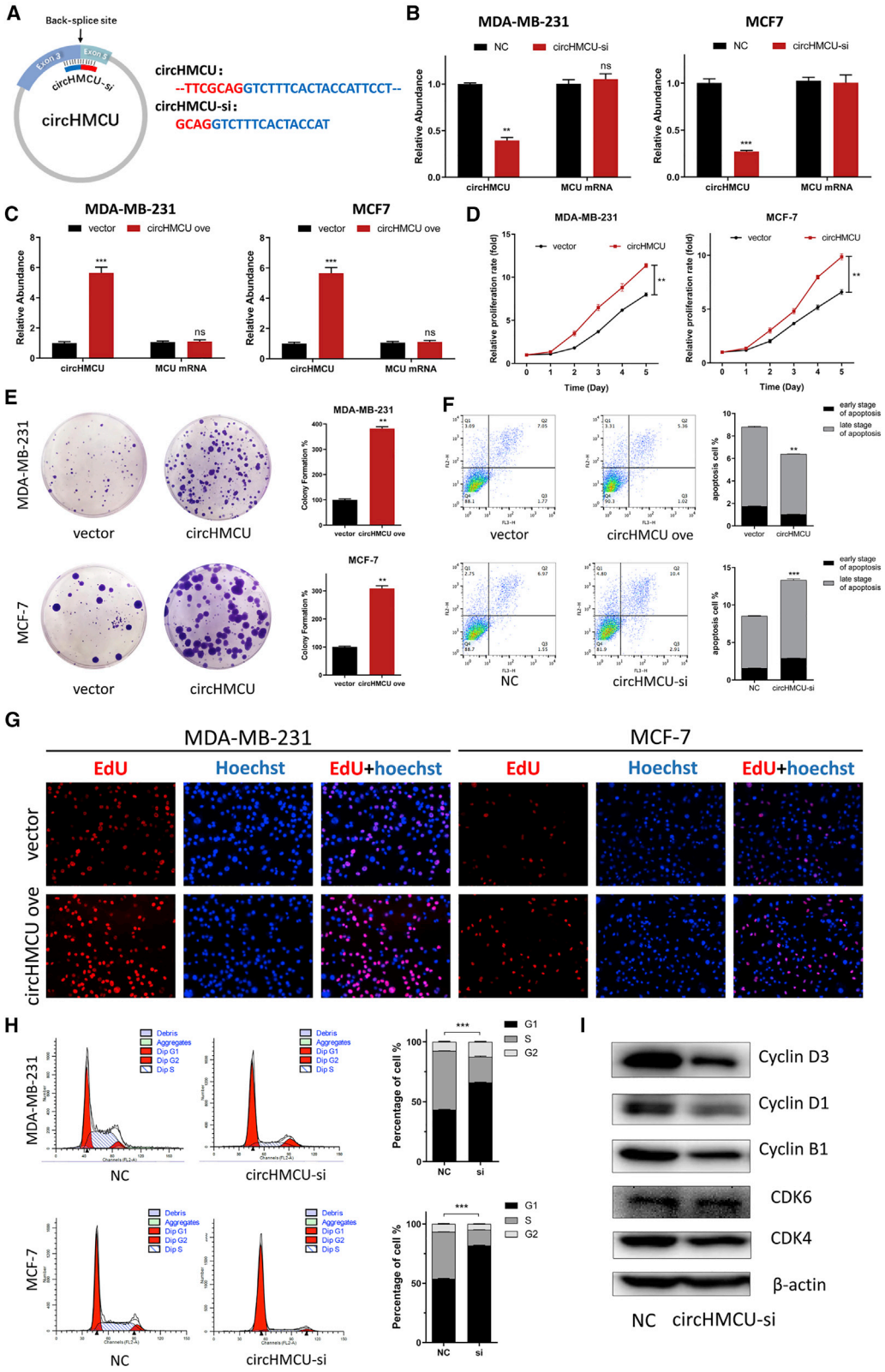

(legend on next page)

Furthermore, the MTT assay showed that overexpression of the MCU linear isoform could not promote the proliferation of breast cancer cells (Figure S3A), suggesting that the cancer-promoting effect in Figure 2 was due to circHMCU but not MCU linear isoform. Taken together, these results suggested that circHMCU could play important roles in promoting cell proliferation in breast cancer cells.

circHMCU Promoted Migration and Invasion Abilities via Modification of the EMT Pathway

To investigate the role of circHMCU on the metastatic ability of breast cancer cells *in vitro*, we transfected cells with circHMCU-si and an NC, and a Transwell system was used to examine the change of migration and invasion ability of cells. As shown in Figures 3A and 3B and S2D, the cell counts of MDA-MB-468, MDA-MB-231, and SKBR3 were significantly decreased in both migration and invasion assays after transfection with circHMCU-si compared with the NC groups, which suggested that circHMCU could promote the metastatic ability of breast cancer cells. Consistently, circHMCU overexpression enhanced the migration and invasion abilities of MDA-MB-231, MDA-MB-468, and SKBR3 cells, indicating that circHMCU could promote cancer cell metastasis regardless of the hormone receptor and HER2 status. However, linear isoform of MCU could not promote migration and invasion abilities in breast cancer cells (Figure S3B). Taken together, these results suggested that circHMCU may act as a tumor promoter by enhancing metastasis ability of cancer cells. By further exploration of the mechanism of circHMCU on cell motility, we found that circHMCU could modify the epithelial-mesenchymal transition (EMT) pathway, which promoted mesenchymal phenotypes and inhibited epithelial phenotypes (Figure 3D). We examined the expression of epithelial and mesenchymal markers in circHMCU overexpression and control cells. After transfection with circHMCU overexpression plasmid, the epithelial marker E-cadherin was downregulated, whereas ZEB1, fibronectin, and N-cadherin were significantly upregulated (Figure 3C). In conclusion, circHMCU could enhance the migration and invasion of breast cancer cells via promoting the EMT pathway.

circHMCU Acts as a miRNA Sponge for the let-7 Family in Breast Cancer Cells

In order to further explore the underlying mechanism of the cancer-promoting function of circHMCU, bioinformatics analysis was performed and revealed that circHMCU may interact with several miRNAs and therefore regulate the expression level of their downstream target genes (Figures 4A and 4C). According to StarBase, a total of 20 miRNAs were predicted that could be bound to circHMCU, and 9 of them belonged to the let-7 family. We further analyzed the association of these potential miRNA expressions with patient prognosis using The Cancer Genome Atlas (TCGA) and the GEO database. Among them, a high expression level of let-7 family miRNAs was associated with better overall survival in breast cancer patients (Figure 4B). Bioinformatics analysis showed that the two putative complementary binding sites for let-7 with starting nucleotides at positions 30 and 388 in circHMCU were both a 7-mer-1a seed match type with strong compensatory base-pairing for the 5′ end of the let-7 family (Figure 4D). It was reported that miRNAs function as components of ribonucleoprotein (RNP) complexes or RNA-induced silencing complexes (RISCs), and Argonaute 2 (AGO2) was one of the most important and best characterized components of RISCs.[10] A RNA immunoprecipitation (RIP) assay was performed to confirm whether circHMCU was associated with miRNA RNP (miRNP). As shown in Figure 4E, circHMCU and let-7 miRNAs were significantly enriched in AGO2-containing miRNPs relative to control immunoglobulin G (IgG) immunoprecipitates, whereas β-actin mRNA did not detectably associate with the miRNPs. HMGA2, MYC, and CCND1 are target genes of the let-7 miRNAs family, which could be downregulated by let-7. The results of qRT-PCR showed a lower expression level of the let-7 family and higher expression of let-7 target genes (HMGA2, MYC, CCND1) in 4175 and SCP2 cells in which circHMCU was highly expressed (Figure 4F). Moreover, the expression of let-7 miRNAs or let-7 target genes pulled down with anti-AGO2 antibodies in the circHMCU-overexpressing group was significantly higher or lower compared to the control group, respectively (Figure S4), suggesting that circHMCU could inhibit the association between let-7 and its targets in an AGO2 manner, thus verified our hypothesis that circHMCU could act as a let-7 miRNA sponge.

Luciferase reporter assays were used to determine whether circHMCU could bind directly to the miRNAs let-7 family. The structure of the vector used in the luciferase reporter assays is shown in Figure 4G. The plasmid pmirGLO-let-7 4x, which harbored four copies of let-7 binding sites in the 3′ UTR of the firefly luciferase reporter gene (luc2), was used as positive control. The fragment of circHMCU harboring predicted binding site with starting nucleotide at positions 30 and 388 or the mutant binding site were cloned to pmirGLO plasmid and used in luciferase reporter assays (Figure 4H). As expected, cotransfected let-7 mimics and pmirGLO-let-7 4x inhibited luc2 expression in a dose-dependent manner (Figure 4I). A

Figure 2. Effects of circHMCU on Breast Cancer Cell Cycle, Proliferation, and Apoptosis *In Vitro*

(A) Schematic illustrating the target sequences of the siRNAs specific to the back-splicing junction of circHMCU. (B) The expression levels of circHMCU in MDA-MB-231 cells transfected with NC (negative control) or circHMCU-si were detected by real-time PCR. (C) The expression levels of circHMCU in MDA-MB-231 cells after stable transfection of circHMCU or empty vector plasmids were detected by real-time PCR. (D) MTT assays were used to determine the cell viability of MDA-MB-231 and MDA-MB-468 cells transfected with circHMCU overexpression plasmid. (E) A colony formation assay was performed in MDA-MB-231 and MDA-MB-468 cells stably transfected with circHMCU overexpression plasmid. (F) The overexpression of circHMCU decreased apoptosis in MDA-MB-468 cells. (G) Observation of DNA synthesis of MDA-MB-231 and MDA-MB-468 cells transfected with circHMCU overexpression plasmid by EdU assay. (H) Flow cytometry was performed to determine the effect of circHMCU on changes in cell cycle distribution (left). Statistical diagrams show significant differences (middle). Western blotting was used to detect cyclin B1, cyclin D1, cyclin D3, CDK4, and CDK6 expression (left). Data are the means ± SEM of three experiments. $^{**}p < 0.01$, $^{***}p < 0.001$.

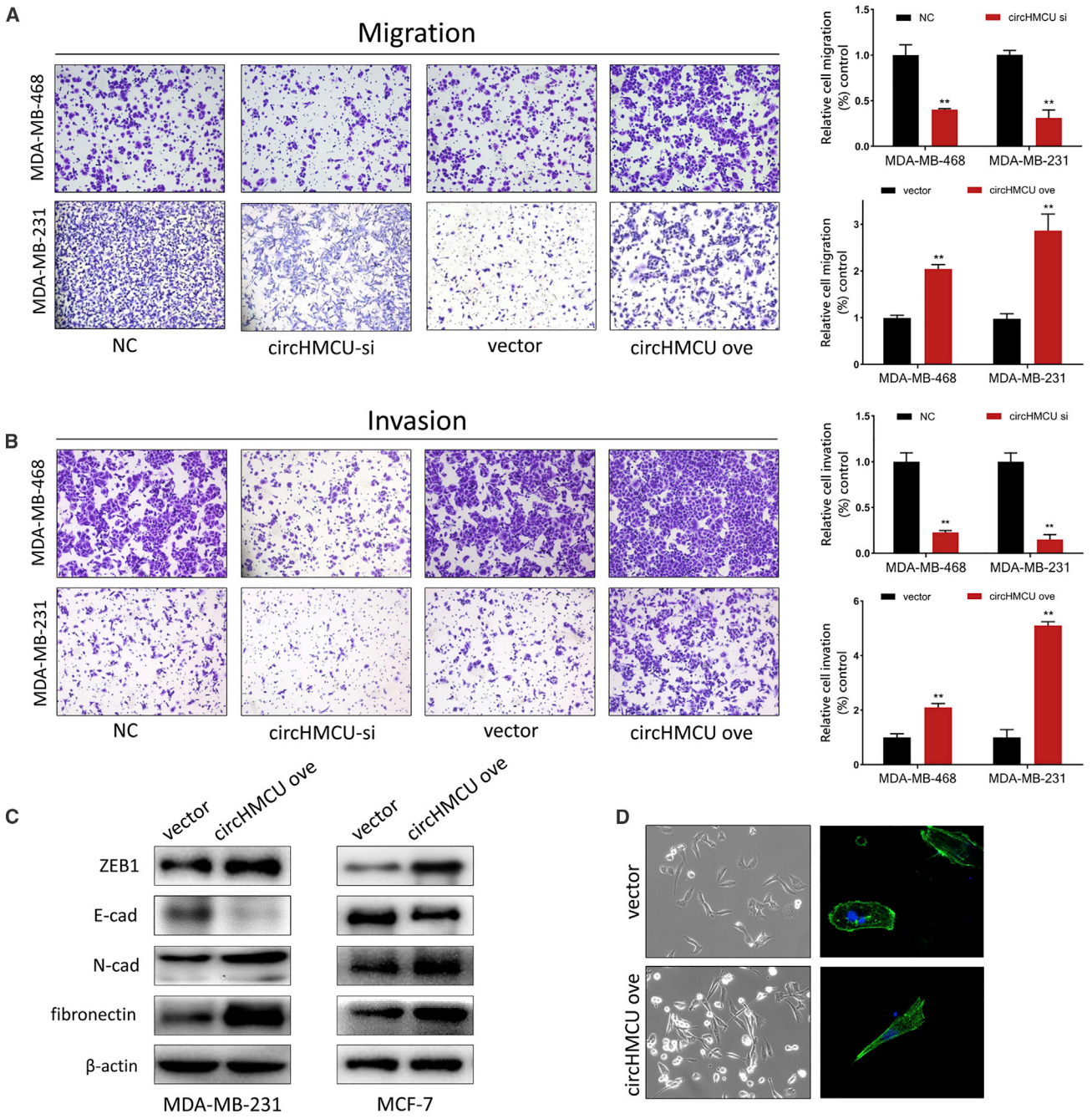

Figure 3. circHMCU Promoted Migration and Invasion Abilities via Modification of the EMT Pathway

(A) Transwell migration assays demonstrated that circHMCU knockdown inhibited cell migration while circHMCU overexpression enhanced the migration ability of MDA-MB-231 and MDA-MB-468 cells. The columns are the average of three independent experiments. (B) Transwell invasion assays demonstrated that circHMCU knockdown inhibited cell invasion while circHMCU overexpression enhanced the invasion ability of MDA-MB-231 and MDA-MB-468 cells. The columns are the average of three independent experiments. (C) circHMCU overexpression led to increased N-cadherin, fibronectin, ZEB1 expression, and decreased E-cadherin expression in MDA-MB-231 and MCF-7 cell lines. (D) The stable overexpression of circHMCU induced morphological changes in MDA-MB-231 cells. Data are the means ± SEM of three experiments. $^{**}p < 0.01$, $^{***}p < 0.001$.

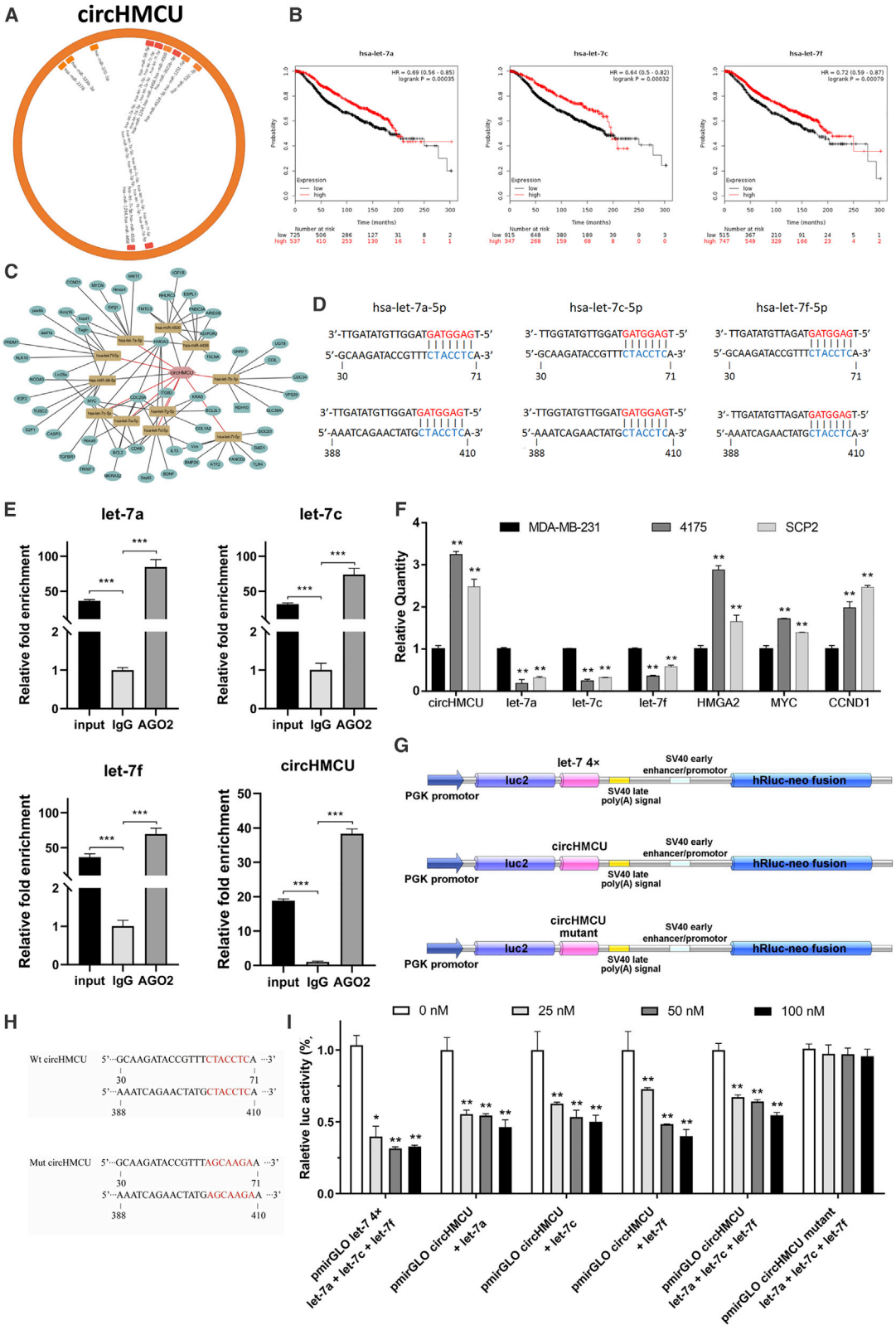

(legend on next page)

dose-dependent inhibition was also observed with pmirGLO-circHMCU. let-7a, let-7c, and let-7f were chosen to tested individually and dose-dependent inhibitions were evident as well. In addition, when transfected with mutant vectors that contained the circHMCU fragment with mutations at two putative let-7 binding sites, the let-7 mimic caused no obvious change in luciferase activity, confirming that the observed inhibition was dependent on the predicted let-7 sites.

let-7 Mimics Block the Tumor-Promoting Effects of circHMCU Overexpression by Downregulating HMGA2, MYC, and CCND1

Given that circHMCU serves as a sponge of let-7 and that circHMCU plays a promoting role in breast cancer, we sought to determine whether let-7 counteracted circHMCU to inhibit the development and progression of breast cancer. A migration assay and wound healing assay were performed to detect the metastatic potency of breast cancer cells. We co-transfected a circHMCU overexpression vector with let-7 mimics into the cells. As shown in Figure 5A, let-7 suppressed the circHMCU-induced increase in the migration capacity of the breast cancer cells. Consistently, let-7 blocked the circHMCU-induced increase of wound healing ability in breast cancer cells (Figure 5B). In addition, an EdU incorporation assay (Figure 5C) and MTT assay (Figure 5D) were performed and the enhanced cell proliferation rate of the circHMCU overexpression group was significantly abrogated by the co-expression of let-7 mimics. Given that MYC, HMGA2, and CCND1 were reported as the downstream target genes of let-7, we next investigated whether circHMCU exerts its promoting effect by modulating the expression of MYC, HMGA2, and CCND1. As shown in Figure 5F, overexpression of circHMCU could increase the protein level of MYC, HMGA2, and CCND1. Additionally, the combined transfection of circHMCU and let-7 mimics was conducted and we found that let-7 partly rescued the promoting effect of circHMCU on the expression of MYC, HMGA2, and CCND1, which agreed with the results of cell function. Furthermore, Kaplan-Meier survival plots were computed using the datasets from TCGA database, and the results showed that high expression of MYC and CCND1 contributed to worse overall survival (OS), disease-free survival (DFS), and distant metastasis-free survival (DMFS) in breast cancers (Figure 5E). HMGA2, one of the let-7 target genes, was reported to be a driver of tumor metastasis. Worse OS, DFS, and DMFS were associated with HMGA2 expression in breast cancer patients with positive lymph nodes (Figure 5E). However, no significant association was found in breast cancer patients with all lymph node states (Figure S5), indicating that HMGA2, as a target gene of let-7, played an important role in the metastasis of breast cancer. These findings further demonstrated that upregulation of MYC, HMGA2, and CCND1 by the circHMCU/let-7 family worsened the prognosis of breast cancer patients, which suggested that circHMCU plays an important role in the regulation of progression and metastasis of breast cancer.

circHMCU Promoted Breast Cancer Cell Growth and Metastasis in a Xenograft Model

Our results have validated that overexpression of circHMCU promoted cell growth and metastasis of breast cancer cell lines *in vitro*. To further explore the role of circHMCU, MDA-MB-231 was chosen to be transfected with pLCDH-ciR (NC) and pLCDH-ciRHMCU (circHMCU overexpression) because of its highly tumorigenic and metastatic abilities. MDA-MB-231 breast cancer cells were subcutaneously injected into the right flank of BALB/c nu/nu mice. As shown in Figures 6A and 6C, xenograft tumor growth and tumor volume were significantly increased in the circHMCU overexpression group as compared to the NC group. RT-PCR was performed to verify the overexpression efficiency of MDA-MB-231 stable cells in xenograft tumors (Figure 6B). Lung metastasis was reported to be an indicator of tumor aggressiveness and was tested in our study to validate the function of circHMCU. As shown in Figure 6D, metastasis of the circHMCU overexpression group was significantly increased compared to the control group, which was also demonstrated by H&E staining assay (Figure 6E). To validate the regulatory function of circHMCU on let-7 target genes, the expression levels of MYC, HMGA2, CCND1, and Ki-67 were examined by immunohistochemistry (IHC). The results showed that, compared to NCs, the expression of MYC, HMGA2, CCND1, and Ki-67 significantly decreased (Figure 6F; Figure S6). Furthermore, tissues from breast cancer patients were strained by IHC in order to verify our conclusion. We found that in patients with high circHMCU, the expression levels of MYC, HMGA2, and CCND1 were significantly higher compared with patients with low circHMCU (Figure 6G). These results demonstrate that circHMCU can promote breast cancer progression *in vivo* and increase the expression of MYC, HMGA2, and CCND1.

DISCUSSION

Breast cancer is a type of highly heterogeneous disease and the underlying oncogenic mechanisms have been increasingly elucidated in recent years. During the past decades, increasing numbers of non-coding RNAs have been identified, including miRNAs, long non-coding RNAs (lncRNAs), and circRNAs. Accumulating evidence has

Figure 4. circHMCU Acts as a miRNA Sponge for the let-7 Family in Breast Cancer Cells

(A) Schematic model showing the putative binding sites for miRNAs and circHMCU. (B) Kaplan-Meier analysis revealed that the expression of the let-7 family was positively correlated with survival of breast cancer patients. (C) ceRNA analysis for circHMCU. Cytoscape was used to visualize circHMCU-miRNA-target gene interactions based on the bioinformatics analysis of StarBase. In the network, 11 miRNAs and the 56 most possible target genes of these miRNAs were collected. The hexagon represents circHMCU, the round rectangles represent miRNAs, and the circles represent target genes of miRNAs. The relationships between the nodes are connected with solid lines. (D) Schematic representation of potential binding sites of let-7 microRNAs with circHMCU. (E) AGO2 RNA immunoprecipitation (RIP) assay for the enrichment of circHMCU and let-7 microRNAs in 293T cells. The expression levels of circHMCU and let-7 microRNAs were detected using quantitative real-time PCR. (F) Relative expression levels of circHMCU, let-7 microRNAs, and their target genes in MDA-MB-231, 4175, and SCP2 cell lines. (G) Schematic representation of reporter constructs used in luciferase reporter assay. (H) Schematic representation of mutated nucleotides of two complementary site in circHMCU. (I) Luciferase activity of wild-type circHMCU or mutant circHMCU after transfection with let-7 microRNA mimics or NC (negative control) in HEK293T cells. Data are the means ± SEM of three experiments. *$p < 0.05$, **$p < 0.01$, ***$p < 0.001$.

shown the important roles of non-coding RNAs in epigenetic regulation of various kind of diseases, especially cancers.[11–13] circRNA is a newly identified type of non-coding RNA molecule with 3′ and 5′ ends covalently linked in a closed-loop structure. The expression of circRNAs has been widely detected in a large number of metazoans and in diverse cell types and organisms. The processing of circRNAs was reported to be facilitated by either RNA pairing of reversely complementary sequences across their flanking introns[3] or protein factors (such as MBL and RBM3) binding to precursor (pre-)mRNAs to bridge flanking introns together.[14,15] The high stability, high conservation, and tissue specificity of circRNAs suggested that circRNAs may play a key role in the development of human diseases. Recent studies have reported that some circRNAs could serve as regulators in breast cancer, such as circ-ABCB10,[16] hsa_circ_0001982,[17] circRNA-000911,[18] and circGFRA1[19]. However, the function of circRNAs and their underlying mechanisms remain largely unknown. In the present study, we found circHMCU to be upregulated in breast cancer cell lines with high metastatic ability and breast cancer tissues. Further analyses were conducted to determine preliminarily the biological functions and molecular mechanism of the newly identified circHMCU.

The ceRNA hypothesis proposes that transcripts with shared miRNA binding sites (usually different types of coding and non-coding members of the transcriptome) compete in a post-transcriptional regulatory network. In recent decades, numerous studies have supported this hypothesis, and it has gained substantial attention as a unifying function for lncRNAs, pseudogene transcripts, and circRNAs.[20] Stable transcripts such as circRNAs with a host of miRNA-binding sites or MREs can function as miRNA sponges. A circRNA named ciRS-7, which contains more than 70 MREs, was first reported to function as a sponge of miR-7.[21] However, only a few circRNAs or ceRNAs have multiple binding sites for a particular miRNA, with most of them containing only one or two miRNA binding sites. In the present study, we found that circHMCU promoted proliferation, migration, and invasion of human breast cancer cells by targeting the let-7 family, which has not been reported by previous studies. Furthermore, we demonstrated that two binding sites were critical for circHMCU to sponge let-7. let-7 serving as a regulator in the progression of cancer has been reported in several models, including ovarian cancer,[22] prostate cancer,[23] lung cancer,[24] and breast cancer.[25] As tumor suppressors, let-7 miRNAs repress several oncogenes, including MYC,[26] HMGA2,[27] and CCND1,[28] which were associated with enabling replicative immortality, invading growth suppressors, and activating metastasis in the development and progression of cancer. HMGA2 was reported to play a critical role in EMT by activating the transforming growth factor β (TGF-β) signaling pathway, thereby inducing invasion and metastasis of human epithelial cancers.[29] CCND1, bound with its partners CDK 4/6, partially mediated G_1/S phase transition of the cell cycle through phosphorylation and inactivation of retinoblastoma (Rb) protein with subsequent release of E2F transcription factors, and thus promoted cell proliferation.[30] MYC could modulate the intrinsic apoptotic pathway by altering the balance of proapoptotic and antiapoptotic members of the Bcl-2 family, in parallel with or independent of p53.[31] In our study, we found that let-7 could bind to circHMCU and thus affect target genes of let-7 (MCY, HMGA2, and CCND1), suggesting that circHMCU may function as a let-7 sponge to modulate breast cancer proliferation and metastasis via regulating the expression of MCY, HMGA2, and CCND1. Of note, not all circRNAs can act as "miRNA sponges." For example, some circRNAs can regulate transcription and alternative splicing, interact with RNA-binding proteins (RBPs), and even be absorbed into exosomes and function as promising biomarkers for cancer diagnosis. Thus, further specific studies are needed to decipher whether circHMCU plays a role in some other pathological process in breast cancer progression.

In conclusion, we found that circHMCU was upregulated in human breast cancer, which could remarkably promote proliferation and metastasis of breast cancer cells. We further found that circHMCU could efficiently sponge the let-7 family to increase the expression of MYC, HMGA2, and CCND1. Our findings provided a novel circHMCU/let-7 family/target genes (MYC, HMGA2, and CCND1) axis that broadens our insights into the underlying mechanisms of breast cancer and provides new biomarkers and potential therapeutic targets in the clinic.

Conclusions

In summary, our study found a circRNA, circHMCU, that was upregulated in breast cancer tissues and correlated with poor prognosis. Further study revealed that circHMCU could significantly promote proliferation and metastasis abilities of breast cancer cells both *in vitro* and *in vivo*. Mechanistically, we found that circHMCU could function as a miRNA sponge for the let-7 family, which was validated by RIP and luciferase reporter assays. The let-7 family is a well-known tumor suppressor because of its formidable function and is considered as a potential diagnostic and prognostic marker. Our study identified circHMCU as a miRNA sponge of the let-7 family that has important significance in understanding the regulatory function of let-7 in breast cancer.

MATERIALS AND METHODS

Cell Culture

Human breast cancer cells (MDA-MB-231, MDA-MB-468, and MCF7) were purchased from the American Type Culture Collection (Manassas, VA, USA). The cell lines were characterized by Genetic Testing Biotechnology Corporation (Suzhou, China) using short tandem repeat markers. Cells were routinely cultured in Dulbecco's modified Eagle's medium (Gibco-BRL, Rockville, IN, USA) supplemented with 10% heat-inactivated fetal bovine serum (HyClone), 100 U/mL penicillin, and 100 μg/mL streptomycin. Cells were maintained at 37°C in a humidified atmosphere with 5% CO_2.

Tissue Specimens and Ethics Statement

Studies using human tissues were reviewed and approved by the Ethics Committee of Shandong University. Breast cancer tissues and adjacent normal breast tissues were obtained from patients who were diagnosed with breast cancer and had undergone surgery

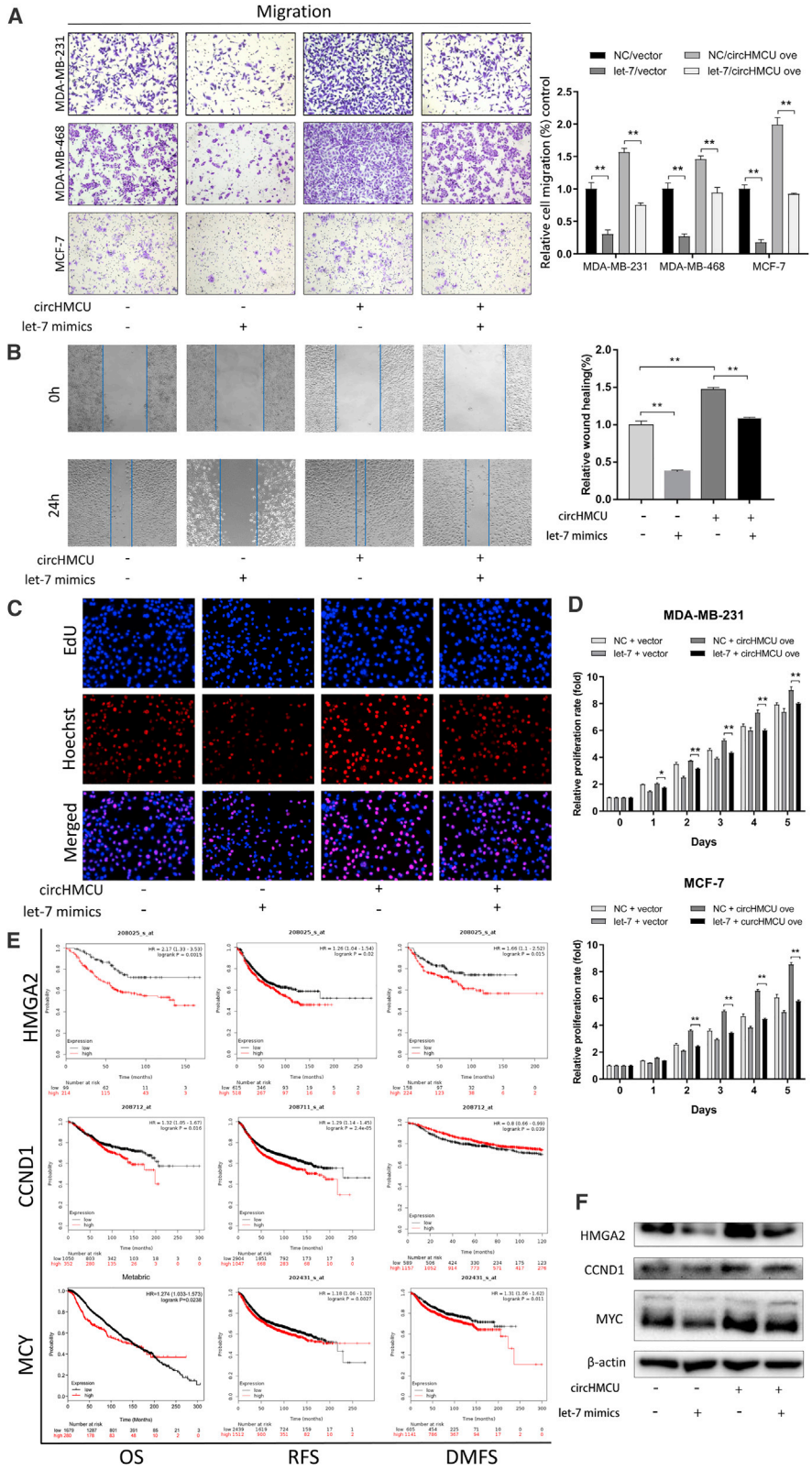

(legend on next page)

from July 2008 to January 2015 in Qilu Hospital of Shandong University. The median follow-up is 78 months. Tissue samples were stored at −80°C until RNA extraction. Histological and pathological diagnoses were confirmed. All of the participants in this study provided written informed consent for the use of the clinical materials obtained in the study.

Gene Expression Profiles

The gene expression data matrix of parental MDA-MB-231 (231-PAR) cells and lung metastatic cells (LM2) was obtained from the National Center for Biotechnology GEO database (https://www.ncbi.nlm.nih.gov/geo/), which is accessible through the GEO platform GPL21825 (GEO: GSE111504). In the present study, we selected the data of parental MDA-MB-231 cells and lung metastatic cells (LM2) for further study. Data analysis was performed with R software.

RNA Extraction and Quantitative Real-Time PCR

Total RNA was prepared from cell lines using TRIzol reagent (Invitrogen, CA, USA) according to the manufacturer's instructions. For circRNAs, RNase R was used to degrade linear RNAs, which have poly(A), and amplified by divergent primer. Total RNA (2 μg) was incubated for 30 min at 37°C with 3 U/μg RNase R. Reverse transcription was performed with the PrimeScript RT reagent kit (Takara, Japan), and quantitative real-time PCR was performed using a SYBR Green PCR kit (Takara, Japan). β-Actin was used as an endogenous control. Nuclear and cytoplasmic fractions were isolated using the PARIS kit (Life Technologies, Carlsbad, CA, USA) following the manufacturer's instructions.

ActD Treatment

Transcription was prevented by the addition of 2 mg/mL ActD or DMSO (Sigma-Aldrich, St. Louis, MO, USA) as the NC to the cell culture medium. After treatment in the indicated time, the RNA expression levels of circHMCU and MCU were detected by qRT-PCR.

Plasmid Construction and Cell Transfection

In order to induce MCU transcript formation *in vitro* by nonlinear splicing, the circHMCU overexpression vector was constructed. The cDNA encoding circHMCU in MCF7 cells (including exons 3 and 4 and introns 3 and 4 between them) with a length of 292 bp was amplified and the fragment was cloned to the pLCDH-ciR vector (Guangzhou Geenseed Biotech, Guangzhou, China) between the two specially designed front and back circular frames that were on the vector. The primer sequences used for circHMCU-overexpressed vector were as follows: forward, 5′-CGGAATTCTGAAATATGCTATCTTACAGGTCTTTCACTACCATTCCTACAGTG-3′, reverse, 5′-CGGGATCCTCAAGAAAAAATATATTCACCTGCGAATGTTCAAGTTTCCCCT-3′. The result of vector construction was verified by direct sequencing. The expression plasmid vector and the empty vector were used to transfect breast cancer cells using Lipofectamine 2000 (Invitrogen, MA, USA) in order to establish the circHMCU overexpression and control cell lines. For circHMCU knockdown, circHMCU-si and and si-NC were purchased from Ribobio (Guangzhou, China). The sequence of the functional circHMCU-si was 5′-GCAGGTCTTTCACTACCAT-3′ and 5′-UUCUCCGAACGUGUCACGU-3′ for the NC. Transfections were performed using Lipofectamine 2000 to establish the si-NC and circHMCU-si cell lines.

Protein Isolation and Western Blot

Cells were harvested and lysed with lysis buffer (1× PBS, 1% Nonidet P-40 [NP40], 0.1% sodium dodecyl sulfate, 0.5% sodium deoxycholate, 5 mM ethylenediaminetetraacetic acid, and 1 mM sodium orthovanadate) containing protease inhibitors. 10% SDS-PAGE was used to separate protein extracts. After electrophoresis, protein extracts were transferred onto polyvinylidene fluoride membranes (Bio-Rad, Hercules, CA, USA) in 200 mA for 2 h, followed by blocking with 5% non-fat milk for another 1 h. The membranes were incubated with primary antibodies at 4°C overnight and labeled with horseradish peroxidase-coupled secondary antibodies for 2 h at room temperature. The protein bands were detected with enhanced chemiluminescence. The expression of β-actin was used as the endogenous control.

MTT Assay

After transfection, cells were seeded in 96-well plates with 1,000 cells per well. 20 μL of MTT solution (5 mg/mL) was added to each well and incubated for 4–6 h at 37°C. We recorded the optical density (OD) value immediately and at 24, 48, 72, 96, and 120 h after transfection for statistical analysis. Each experiment was performed in triplicate.

Cell Cycle Assay

Forty-eight hours after transfection with si-NC or circHMCU-si, the cells were trypsinized and washed with cold PBS twice. Then, the cells were suspended with 300 mL of PBS, followed by the addition of 500 mL of cell cycle staining buffer (Multi Sciences [Lianke] Biotech). A flow cytometer (Becton Dickinson, NJ, USA) was used to analyze the DNA contents of the cells after 30 min of incubation at room temperature, and the data were analyzed with ModFit LT v2.0 software (Becton Dickinson). Each experiment was performed in triplicate.

Figure 5. let-7 Mimics Block the Tumor-Promoting Effects of circHMCU Overexpression by Downregulating HMGA2, MYC, and CCND1

(A) Transwell assays of cell migration after transfection with circHMCU and let-7 mimics in MDA-MB-231, MDA-MB-468, and MCF-7 cells. (B) Wound healing assays after transfection with circHMCU and let-7 mimics in MDA-MB-231 cells. (C) Observation of DNA synthesis of MCF-7 cells transfected with circHMCU overexpression vectors and let-7 mimics by EdU assay. (D) MTT analysis of cell proliferation after transfection with circHMCU overexpression vectors and let-7 mimics in MDA-MB-231 and MCF-7 cells. (E) Kaplan-Meier survival curve shows the relationship between HMGA2/CCND1/MYC expression and survival rates of breast cancer patients. (F) Western blot analysis of the expression levels of HMGA2, MYC, and CCND1 after transfection with circHMCU and let-7 in MDA-MB-231 cells. Data are the means ± SEM of three experiments. *$p < 0.05$, **$p < 0.01$

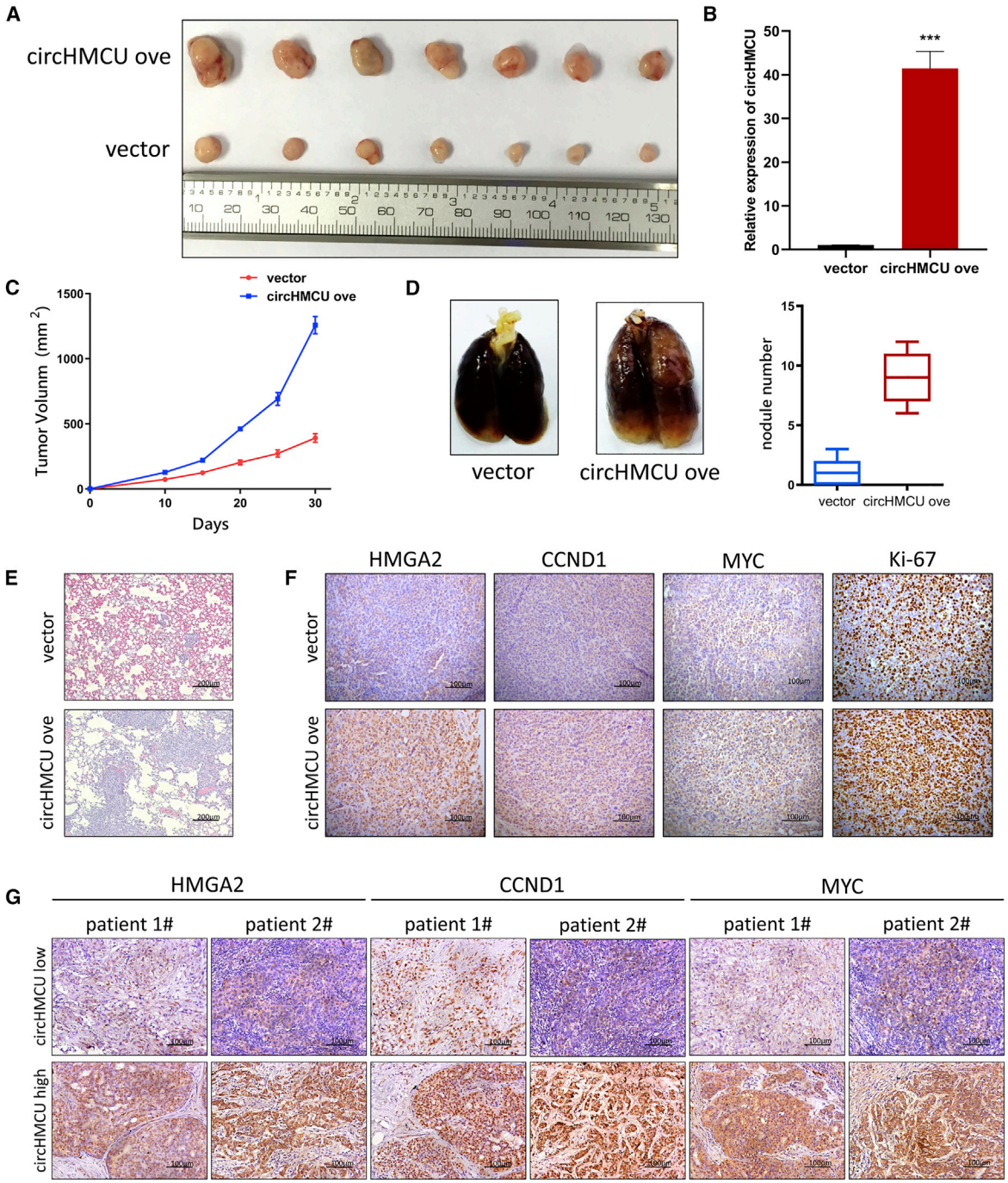

Figure 6. circHMCU Promoted Breast Cancer Cell Growth and Metastasis in a Xenograft Model

(A) Photograph illustrated tumors in xenografts. Overexpression of circHMCU promoted the growth of tumors. (B) Expression of circHMCU in the xenograft model. (C) Growth curve of xenograft tumors after tumor cells injection. (D) Overexpression of circHMCU promoted lung metastasis of MDA-MB-231 cells. (E) Representative images of hematoxylin and eosin (H&E) staining of lungs isolated from mice that received tail vein injection of MDA-MB-231 pLCDH-ciR (empty vector) cells and circHMCU overexpression cells. Scale bars, 200 μm. (F) IHC staining analysis revealed the increased expression of proliferation index Ki-67 and HMGA2/MYC/CCND1 expression in circHMCU overexpressed tumors compared with control group. Scale bars, 100 μm. (G) IHC staining analysis of the expression of HMGA2/MYC/CCND1 in the tissues of breast cancer patients with different circHMCU expression levels. Scale bars, 100 μm. Data are the means ± SEM of three experiments. ***$p < 0.001$.

Cell Apoptosis Assay

Cell apoptosis was performed using a phycoerythrin (PE)-annexin V apoptosis detection kit (BD Biosciences, USA) according to the manufacturer's protocols. Briefly, cells were digested with EDTA-free trypsin, centrifuged, and resuspended with 400 μL of annexin binding buffer at a concentration of 10^6 cells/mL. Then, 5 μL of fluorescein isothiocyanate (FITC)-conjugated annexin V and 5 μL of propidium iodide (PI) were added to the cells and incubated at room temperature for 15 min in dark. Within 1 h after staining, a cell apoptosis assay was performed on a flow cytometer (Becton Dickinson, NJ, USA). Each experiment was performed in triplicate.

Cell Invasion and Migration Assays

Migration and invasion assays were performed using the Transwell system (8-mm pore, Corning Life Sciences/Costar, Lowell, MA, USA). For migration assays, 700 μL of medium with 20% fetal bovine serum was added to the lower well of each chamber, and 1×10^5 cells suspended in serum-free medium were added to the upper inserts. After 24–48 h of incubation, the noninvasive cells in the top chambers were removed with cotton swabs, whereas the cells adhering to the lower surface of the membrane were fixed with methanol and stained with 0.1% crystal violet. The total number of cells adhering to the lower surface of the membrane was quantified in six representative fields after incubation for the indicated time. The invasion assay was performed in the same way as the migration assay except that the membrane was coated with Matrigel (BD Biosciences, Bedford, MA, USA). Each experiment was performed in triplicate.

Wound Healing Assay

Cells were seeded onto 24-well plates and transfected with pLCDH-ciR or circHMCU overexpression plasmid for 24 h. When the cells reached 80%–90% confluence, an artificial wound was carefully created by scratching the confluent cell monolayer with a 10-μL pipette tip. The wound was imaged immediately and at 24 h. Each experiment was performed in triplicate.

Colony Formation Assay

The stable cells were generated from MDA-MB-231 and MDA-MB-468 cells transfected with circHMCU overexpression plasmid, and transfection efficiency was confirmed by qRT-PCR. The cells were trypsinized, and 500 cells were plated in 60-mm plates and incubated at 37°C for 20 days. Colonies were fixed with methanol and dyed with dyeing solution containing 0.1% crystal violet. The number of colonies was counted. Each experiment was performed in triplicate.

EdU Incorporation Assay

Cells were seeded in 96-well plates at 20,000 per well 24 h after transient transfection (in the logarithmic phase of growth) and incubated at 37°C in a humidified 5% CO_2 atmosphere for 12 h. Then a Cell-Light EdU DNA cell proliferation kit (Ribobio, Guangzhou, China) was used to monitor the proliferation of breast cancer cells according to the manufacturer's instructions. A fluorescence microscope (Olympus, Tokyo, Japan) was used to count cells in the proliferating phase (excitation, bright red spots) and the total cells (shown in blue).

Luciferase Reporter Assay

For the luciferase reporter assay, pmirGLO Dual-Luciferase vectors (Promega, Madison, WI, USA) were used to construct Dual-Luciferase reporter plasmids. Sequences of circHMCU containing two complementary binding site for let-7 miRNAs were cloned into the vectors. HEK293T cells were co-transfected with wild-type pmirGLO-circHMCU or the mutated type and let-7 mimics or NC using Lipofectamine 2000 (Invitrogen). After induction for 48 h, luciferase activity was assessed using the Dual-Luciferase reporter kit (Promega, Madison, WI, USA). The relative firefly luciferase activity was normalized to Renilla luciferase activity.

RIP Assay

A Magna RIP kit (Millipore, Billerica, MA, USA) was used for RIP experiments according to the manufacturer's instructions. Briefly, 1×10^7 cells at 80% confluence were harvested and then lysed in RIP lysis buffer. After that, 100 μL of cell lysate was incubated with RIP buffer containing magnetic beads conjugated with human anti-AGO2 antibody or normal mouse IgG (Merck Millipore, USA). The specimens were incubated with proteinase K to segregate immunoprecipitated RNA. The extracted RNAs were further evaluated through quantitative real-time PCR.

Tumor Model and Metastasis Assay *In Vivo*

MDA-MB-231 cells transfected with pLCDH-ciR or circHMCU overexpression plasmid were selected and stable cells were generated.[32] These cells (1×10^7) in 200 μL of PBS/Matrigel (3:1, v/v) were injected subcutaneously into the left flank of 4- to 6-week-old BALB/c nu/nu female mice (seven mice per group). Tumor growth rate was monitored by measuring tumor diameters every 5 days. Both maximum length (L) and width (W) of the tumor were measured using a slide caliper, and the tumor volume was calculated as $^1/_2(L \times W2)$. When mice were killed, tumors were collected for immunohistochemistry. To produce experimental lung metastasis, 2×10^5 cells were injected into the lateral tail veins of 4- to 6-week-old BALB/c nu/nu female mice (five mice for each group). After 2 weeks, all mice were killed under anesthesia. The lungs were collected and fixed in 10% formalin. For tissue morphology evaluation, hematoxylin and eosin (H&E) staining was performed on sections from embedded samples. All animal experiments were performed with the approval of the Shandong University Animal Care and Use Committee.

IHC

The tumor tissues were fixed in 10% neutral-buffered formalin for 24 h. After that, the tissues were paraffin-embedded and then sliced into 4-μm sections for further IHC. Briefly, the sections were deparaffinized and rehydrated, followed by antigen retrieval with pH 6.0 citrate buffer. 3% H_2O_2 was used to inhibit endogenous peroxidase activity, and the sections were incubated with 10% normal goat serum to block non-specific binding. After incubation with anti-MYC antibody, anti-HMGA2 antibody, and anti-CCND1 antibody at 4°C overnight, the sections were washed with PBS and then treated with biotinylated anti-Ig antibody for 30 min and reacted with horseradish

peroxidase (HRP)-conjugated streptavidin. Then, the diaminobenzidine (DAB) substrate system (Maixin Bio, Fuzhou, China) was used, followed by counterstaining with hematoxylin. The images were taken by an Olympus light microscope.

Statistical Analysis

SPSS software (version 18.0) was used for statistical analysis. Two group comparisons were performed with the Student's t test. All of the performed tests were two-sided, and error bars represent the standard error of the mean (SEM) of three experiments. Differences with $p < 0.05$ were considered to be statistically significant.

SUPPLEMENTAL INFORMATION

Supplemental Information can be found online at https://doi.org/10.1016/j.omtn.2020.03.014.

AUTHOR CONTRIBUTIONS

X.S. and Q.Y. designed the study; X.S. and Y. Liang performed all experiments; Y. Li, B.C., Y.S, L.D., H.Z., and Y. Liu collected tissue samples and the clinical data; L.W. and W.Z. analyzed and interpreted the data; X.S. wrote the paper; and C.W. revised the paper. All authors read and approved the final manuscript.

CONFLICTS OF INTEREST

The authors declare no competing interests.

ACKNOWLEDGMENTS

This work was supported by the National Natural Science Foundation of China (81272903 and 81672613); the Key Research and Development Program of Shandong Province (2016GGE2775); the Shandong Science and Technology Development Plan (2016CYJS01A02); and by the Special Support Plan for National High Level Talents ("Ten Thousand Talents Program") to Q.Y.

REFERENCES

1. Torre, L.A., Bray, F., Siegel, R.L., Ferlay, J., Lortet-Tieulent, J., and Jemal, A. (2015). Global cancer statistics, 2012. CA Cancer J. Clin. *65*, 87–108.
2. Cocquerelle, C., Mascrez, B., Hétuin, D., and Bailleul, B. (1993). Mis-splicing yields circular RNA molecules. FASEB J. *7*, 155–160.
3. Jeck, W.R., Sorrentino, J.A., Wang, K., Slevin, M.K., Burd, C.E., Liu, J., Marzluff, W.F., and Sharpless, N.E. (2013). Circular RNAs are abundant, conserved, and associated with ALU repeats. RNA *19*, 141–157.
4. Barrett, S.P., and Salzman, J. (2016). Circular RNAs: analysis, expression and potential functions. Development *143*, 1838–1847.
5. Han, D., Li, J., Wang, H., Su, X., Hou, J., Gu, Y., Qian, C., Lin, Y., Liu, X., Huang, M., et al. (2017). Circular RNA circMTO1 acts as the sponge of microRNA-9 to suppress hepatocellular carcinoma progression. Hepatology *66*, 1151–1164.
6. Zhang, J., Liu, H., Hou, L., Wang, G., Zhang, R., Huang, Y., Chen, X., and Zhu, J. (2017). Circular RNA_LARP4 inhibits cell proliferation and invasion of gastric cancer by sponging miR-424-5p and regulating LATS1 expression. Mol. Cancer *16*, 151.
7. Hansen, T.B., Jensen, T.I., Clausen, B.H., Bramsen, J.B., Finsen, B., Damgaard, C.K., and Kjems, J. (2013). Natural RNA circles function as efficient microRNA sponges. Nature *495*, 384–388.
8. Zheng, Q., Bao, C., Guo, W., Li, S., Chen, J., Chen, B., Luo, Y., Lyu, D., Li, Y., Shi, G., et al. (2016). Circular RNA profiling reveals an abundant circHIPK3 that regulates cell growth by sponging multiple miRNAs. Nat. Commun. *7*, 11215.
9. Yang, C., Yuan, W., Yang, X., Li, P., Wang, J., Han, J., Tao, J., Li, P., Yang, H., Lv, Q., and Zhang, W. (2018). Circular RNA circ-ITCH inhibits bladder cancer progression by sponging miR-17/miR-224 and regulating p21, PTEN expression. Mol. Cancer *17*, 19.
10. Filipowicz, W., Bhattacharyya, S.N., and Sonenberg, N. (2008). Mechanisms of post-transcriptional regulation by microRNAs: are the answers in sight? Nat. Rev. Genet. *9*, 102–114.
11. Lu, J., Getz, G., Miska, E.A., Alvarez-Saavedra, E., Lamb, J., Peck, D., Sweet-Cordero, A., Ebert, B.L., Mak, R.H., Ferrando, A.A., et al. (2005). MicroRNA expression profiles classify human cancers. Nature *435*, 834–838.
12. Lin, C., and Yang, L. (2018). Long noncoding RNA in cancer: wiring signaling circuitry. Trends Cell Biol. *28*, 287–301.
13. Wong, C.M., Tsang, F.H., and Ng, I.O. (2018). Non-coding RNAs in hepatocellular carcinoma: molecular functions and pathological implications. Nat. Rev. Gastroenterol. Hepatol. *15*, 137–151.
14. Ashwal-Fluss, R., Meyer, M., Pamudurti, N.R., Ivanov, A., Bartok, O., Hanan, M., Evantal, N., Memczak, S., Rajewsky, N., and Kadener, S. (2014). circRNA biogenesis competes with pre-mRNA splicing. Mol. Cell *56*, 55–66.
15. Dong, W., Dai, Z.H., Liu, F.C., Guo, X.G., Ge, C.M., Ding, J., Liu, H., and Yang, F. (2019). The RNA-binding protein RBM3 promotes cell proliferation in hepatocellular carcinoma by regulating circular RNA SCD-circRNA 2 production. EBioMedicine *45*, 155–167.
16. Liang, H.F., Zhang, X.Z., Liu, B.G., Jia, G.T., and Li, W.L. (2017). Circular RNA circ-ABCB10 promotes breast cancer proliferation and progression through sponging miR-1271. Am. J. Cancer Res. *7*, 1566–1576.
17. Tang, Y.Y., Zhao, P., Zou, T.N., Duan, J.J., Zhi, R., Yang, S.Y., Yang, D.C., and Wang, X.L. (2017). Circular RNA hsa_circ_0001982 promotes breast cancer cell carcinogenesis through decreasing miR-143. DNA Cell Biol. *36*, 901–908.
18. Wang, H., Xiao, Y., Wu, L., and Ma, D. (2018). Comprehensive circular RNA profiling reveals the regulatory role of the circRNA-000911/miR-449a pathway in breast carcinogenesis. Int. J. Oncol. *52*, 743–754.
19. He, R., Liu, P., Xie, X., Zhou, Y., Liao, Q., Xiong, W., Li, X., Li, G., Zeng, Z., and Tang, H. (2017). circGFRA1 and GFRA1 act as ceRNAs in triple negative breast cancer by regulating miR-34a. Journal of experimental & clinical cancer research. J. Clin. Exp. Cancer Res. *36*, 145.
20. Thomson, D.W., and Dinger, M.E. (2016). Endogenous microRNA sponges: evidence and controversy. Nat. Rev. Genet. *17*, 272–283.
21. Memczak, S., Jens, M., Elefsinioti, A., Torti, F., Krueger, J., Rybak, A., Maier, L., Mackowiak, S.D., Gregersen, L.H., Munschauer, M., et al. (2013). Circular RNAs are a large class of animal RNAs with regulatory potency. Nature *495*, 333–338.
22. Park, S.M., Shell, S., Radjabi, A.R., Schickel, R., Feig, C., Boyerinas, B., Dinulescu, D.M., Lengyel, E., and Peter, M.E. (2007). Let-7 prevents early cancer progression by suppressing expression of the embryonic gene HMGA2. Cell Cycle *6*, 2585–2590.
23. Ozen, M., Creighton, C.J., Ozdemir, M., and Ittmann, M. (2008). Widespread deregulation of microRNA expression in human prostate cancer. Oncogene *27*, 1788–1793.
24. Takamizawa, J., Konishi, H., Yanagisawa, K., Tomida, S., Osada, H., Endoh, H., Harano, T., Yatabe, Y., Nagino, M., Nimura, Y., et al. (2004). Reduced expression of the let-7 microRNAs in human lung cancers in association with shortened postoperative survival. Cancer Res. *64*, 3753–3756.
25. Sempere, L.F., Christensen, M., Silahtaroglu, A., Bak, M., Heath, C.V., Schwartz, G., Wells, W., Kauppinen, S., and Cole, C.N. (2007). Altered microRNA expression confined to specific epithelial cell subpopulations in breast cancer. Cancer Res. *67*, 11612–11620.
26. Sampson, V.B., Rong, N.H., Han, J., Yang, Q., Aris, V., Soteropoulos, P., Petrelli, N.J., Dunn, S.P., and Krueger, L.J. (2007). MicroRNA let-7a down-regulates MYC and reverts MYC-induced growth in Burkitt lymphoma cells. Cancer Res. *67*, 9762–9770.
27. Lee, Y.S., and Dutta, A. (2007). The tumor suppressor microRNA let-7 represses the HMGA2 oncogene. Genes Dev. *21*, 1025–1030.
28. Ricarte-Filho, J.C., Fuziwara, C.S., Yamashita, A.S., Rezende, E., da-Silva, M.J., and Kimura, E.T. (2009). Effects of let-7 microRNA on cell growth and differentiation of papillary thyroid cancer. Transl. Oncol. *2*, 236–241.

29. Morishita, A., Zaidi, M.R., Mitoro, A., Sankarasharma, D., Szabolcs, M., Okada, Y., D'Armiento, J., and Chada, K. (2013). HMGA2 is a driver of tumor metastasis. Cancer Res. *73*, 4289–4299.

30. Kato, J., Matsushime, H., Hiebert, S.W., Ewen, M.E., and Sherr, C.J. (1993). Direct binding of cyclin D to the retinoblastoma gene product (pRb) and pRb phosphorylation by the cyclin D-dependent kinase CDK4. Genes Dev. *7*, 331–342.

31. Hoffman, B., and Liebermann, D.A. (2008). Apoptotic signaling by c-MYC. Oncogene *27*, 6462–6472.

32. Cheng, Z., Yu, C., Cui, S., Wang, H., Jin, H., Wang, C., Li, B., Qin, M., Yang, C., He, J., et al. (2019). circTP63 functions as a ceRNA to promote lung squamous cell carcinoma progression by upregulating FOXM1. Nat. Commun. *10*, 3200.